

Impact of rapid thermal processing on oxygen precipitation in heavily arsenic and antimony doped Czochralski silicon

Xinpeng Zhang, Chao Gao, Maosen Fu, Xiangyang Ma, Jan Vanhellemont et al.

Citation: *J. Appl. Phys.* **113**, 163510 (2013); doi: 10.1063/1.4803061

View online: <http://dx.doi.org/10.1063/1.4803061>

View Table of Contents: <http://jap.aip.org/resource/1/JAPIAU/v113/i16>

Published by the [American Institute of Physics](#).

Additional information on J. Appl. Phys.

Journal Homepage: <http://jap.aip.org/>

Journal Information: http://jap.aip.org/about/about_the_journal

Top downloads: http://jap.aip.org/features/most_downloaded

Information for Authors: <http://jap.aip.org/authors>

ADVERTISEMENT

The advertisement banner for AIP Advances features a green and yellow background with abstract wavy lines. The AIP Advances logo is centered, with 'AIP' in blue and 'Advances' in green, accompanied by a series of orange dots of varying sizes. On the right, a circular seal states 'Now Indexed in Thomson Reuters Databases'. Below the logo, the text 'Explore AIP's open access journal:' is followed by a list of three bullet points: 'Rapid publication', 'Article-level metrics', and 'Post-publication rating and commenting'.

AIPAdvances

Now Indexed in
Thomson Reuters
Databases

Explore AIP's open access journal:

- Rapid publication
- Article-level metrics
- Post-publication rating and commenting

Impact of rapid thermal processing on oxygen precipitation in heavily arsenic and antimony doped Czochralski silicon

Xinpeng Zhang,¹ Chao Gao,¹ Maosen Fu,² Xiangyang Ma,^{1,a)} Jan Vanhellemont,^{1,b)} and Deren Yang¹

¹State Key Laboratory of Silicon Materials and Department of Materials Science and Engineering, Zhejiang University, Hangzhou 310027, People's Republic of China

²Shanxi Materials Analysis and Research Center, School of Materials Science and Engineering, Northwestern Polytechnical University, Xi'an 710000, People's Republic of China

(Received 8 January 2013; accepted 11 April 2013; published online 29 April 2013)

A comparative investigation is performed on the effects of vacancies induced by rapid thermal processing on oxygen precipitation behavior in heavily arsenic- and antimony-doped Czochralski silicon wafers. It is experimentally found that vacancy-assisted oxide precipitate nucleation occurs at 800, 900, and 1000 °C in the Sb-doped wafers, while it only occurs at 800 °C in the As-doped ones. Density functional theory calculations indicate that it is energetically favorable to form AsVO and SbVO complexes in As- and Sb-doped silicon crystals, respectively. These complexes might act as precursors for oxide precipitate nucleation under appropriate conditions. The difference between the effects of rapid thermal processing -induced vacancies on oxide precipitate nucleation in the heavily As- and Sb-doped Cz silicon crystals is tentatively elucidated based on density functional theory calculations revealing the difference in binding energies of AsVO and SbVO complexes. © 2013 AIP Publishing LLC. [<http://dx.doi.org/10.1063/1.4803061>]

I. INTRODUCTION

Oxygen precipitation (OP) in Czochralski (Cz) silicon has been intensively studied during the past half century due to its technological importance in the production of micro-electronic devices.¹ Although OP behavior in lightly doped Cz silicon is well understood, OP in heavily doped n-type Cz silicon has still to be clarified in more detail.

The last decade, rapid thermal processing (RTP) has been widely used to enhance the internal gettering (IG) capability of Cz silicon wafers.^{2,3} It is well documented now that in case of lightly doped Cz silicon, vacancies introduced by RTP at high temperatures significantly enhance OP during subsequent heat treatments.⁴⁻⁸ VO₂ complexes can act hereby as precursors for oxide precipitate nucleation at temperatures up to 1020 °C.^{2,9,10} It has been reported that OP in heavily As or Sb doped n-type Cz silicon is suppressed during conventional thermal annealing.¹⁰⁻¹⁵ Whether the OP enhancement strategy based on RTP can be applied on heavily doped n-type Cz silicon needs to be clarified from a technological point of view. Moreover, it remains an open question whether the aforementioned VO₂-complex-assisted oxide precipitate nucleation mechanism operates also in heavily doped n-type Cz silicon.

It is known that As and Sb have a larger atom size than Si. Therefore, compressive strain arises intrinsically in heavily As- or Sb-doped silicon. As excess vacancies are introduced by RTP, part of this compressive strain can be released by trapping of vacancies by the As or Sb atoms.

Consequently, the formation of VO₂ complexes in heavily As- or Sb-doped Cz silicon will be influenced by the vacancy trapping by the dopant atoms. Furthermore, since on the one hand the atom size of As is smaller than that of Sb, and on the other hand the concentration of As can be much larger than that of Sb in heavily doped Cz silicon, the possible difference between the OP behaviors in heavily As- and Sb-doped Cz silicon crystals after RTP is relevant to be investigated.

In this work, experimental investigations are performed on the OP behavior in heavily As- and Sb-doped Cz silicon crystals subjected to different anneals without and with a prior RTP at high temperature. The aim is to elucidate the effects of RTP-induced vacancies on oxide precipitate nucleation for anneal temperatures ranging from 800 to 1000 °C.

In addition, the vacancy-assisted oxide precipitate nucleation mechanisms operating in heavily As- and Sb-doped Cz silicon crystals are investigated using density functional theory (DFT) calculations. The reason for the different OP behaviors in the two types of heavily doped n-type Cz silicon crystals is specifically addressed from the viewpoint of dopant-vacancy-oxygen complex formation.

II. EXPERIMENTAL

Polished, 150 mm-diameter, <100>-oriented, Cz Si wafers are used in the experiments. The resistivity of the As- and the Sb-doped silicon wafers is about 0.003 and 0.02 Ω cm, respectively. The total O and As concentrations in the 150 mm diameter As doped crystal are about $1.01 \times 10^{18} \text{ cm}^{-3}$ and $2.62 \times 10^{19} \text{ cm}^{-3}$, respectively, as measured by secondary ion mass spectroscopy (SIMS), while for the Sb doped sample, the O and Sb concentrations are $7.5 \times 10^{17} \text{ cm}^{-3}$ and $1.56 \times 10^{18} \text{ cm}^{-3}$, respectively. The

^{a)}Author to whom correspondence should be addressed. Electronic mail: mxyoung@zju.edu.cn

^{b)}On leave from Department of Solid State Sciences, Ghent University, Krijgslaan 281 S1, B-9000 Ghent, Belgium.

dopant concentrations are close to the solubility limit. $1.5 \times 1.5 \text{ cm}^2$ samples are cut from the wafers to be used for the annealing experiments. Half of the samples receive a prior RTP at 1250 °C for 60 s in argon (Ar) ambient. For this RTP treatment, the ramping-up rate is about 100 °C/s and the cooling rate from 1250 to 800 °C is about 50 °C/s. Then, the specimens with and without the prior RTP are divided into three groups, which are annealed at 800 °C for 32 h + 1000 °C for 32 h, at 900 °C for 32 h, and at 1000 °C for 32 h, respectively. All the above anneals are performed in Ar ambient. After annealing, the annealed specimens are etched in Yang 1 etchant [$\text{CrO}_3(0.5 \text{ mol/l})\text{:HF}(49\%) = 1\text{:}1$] for 5 min, followed by optical microscopy (OM) inspection using an Olympus MX-50 microscope equipped with a CCD camera. Moreover, some of the specimens are further characterized by transmission electron microscopy (TEM) in order to study the morphologies of oxide precipitates and the secondary defects associated with the precipitates.

III. DFT CALCULATIONS

DFT calculations are performed with the CASTEP software based on the local density functional (LDA) theory with ultrasoft-pseudopotentials.^{16–18} 64- and 128-atom supercells are used to study the interactions between the substitutional dopant (As or Sb) atom, the vacancy or/and the interstitial oxygen O_i atom with different configurations in silicon lattice. The generalized gradient approximation (GGA) using the Perdew-Burke-Ernzerhof¹⁹ exchange-correlation functional is used. Moreover, a large cutoff energy of 380 eV coupled with a $2 \times 2 \times 2$ (for the 64-atom supercell) and $1 \times 2 \times 2$ (for the 128-atom supercell) Monkhorst-Pack²⁰ scheme for the Brillouin zone sampling is used during structure optimization. The convergence criterion of the structure relaxation was set at 5.0×10^{-6} eV for the energy and at 5.0×10^{-4} Å for the maximum displacement. All the calculation results that are shown were obtained after full convergence.

IV. RESULTS AND DISCUSSION

A. Experimental results

The morphologies of oxide precipitates and the associated secondary defects in the annealed specimens are studied by TEM. Fig. 1 shows typical images of bulk micro-defects (BMDs) in As- and Sb-doped Cz silicon specimens of the present study, subjected to the two-step anneal at 800 °C for 32 h + 1000 °C for 32 h or a single-step anneal at 900 °C for 32 h, both after RTP at 1250 °C for 60 s. In all cases, punched-out dislocations and precipitate-dislocation complexes are observed around the oxide precipitates. This is also the case for the Sb-doped specimen annealed at 1000 °C for 32 h (not shown here). During the anneal at 1000 °C for 32 h, a large amount of silicon self-interstitials are emitted from the growing oxide precipitates and can condense into extended lattice defects. Figure 1(c) shows plate-like oxide precipitates with associated strain fields in the Sb-doped specimen annealed at 900 °C for 32 h. It is known that Sb-doping introduces compressive stress in the silicon lattice

due to the larger atom size. Therefore, the emission of silicon self-interstitials from the growing oxide precipitates is more difficult in Sb doped material, and the stress level in and around the precipitate can be expected to be higher. For that reason the formation of plate-like oxide precipitates is favored as this minimizes the strain energy.^{21,22} In the As-doped samples annealed at 900 or 1000 °C for 32 h, very few precipitates could be found by TEM indicating that no substantial OP occurred, as will be discussed later.

Figures 2 and 3 show OM images of BMDs revealed after preferential etching for the As- and Sb-doped Cz silicon specimens subjected to anneals at 800 °C for 32 h + 1000 °C for 32 h, 900 °C for 32 h, and 1000 °C for 32 h, with and without a prior RTP at 1250 °C for 60 s, respectively. As shown in the upper row of images of Fig. 2, there are hardly any BMDs in the annealed As-doped specimens without prior RTP, indicating a low OP occurred. In the Sb-doped specimens without prior RTP, as shown in the upper row of images of Fig. 3, there is a low density of BMDs, indicating some OP has occurred. With a prior RTP at 1250 °C for 60 s, one observes that: (1) for the As-doped silicon, only the specimen subjected to the anneal at 800 °C for 32 h + 1000 °C for 32 h has a significant density of BMDs, as shown in the lower row of images of Fig. 2, and (2) for the Sb-doped silicon, all the specimens contain a large amount of BMDs. It is known that RTP at 1250 °C introduces a high concentration of vacancies into silicon crystal.^{2,5} In view of the above-mentioned results, one can conclude that vacancy-assisted oxide precipitate nucleation substantially occurs only at 800 °C for the As-doped samples, while it does for the whole temperature range between 800 and 1000 °C for the Sb-doped samples. The different behaviors of the As- and Sb-doped samples can be understood on the basis of DFT calculations as discussed in the next paragraph.

B. DFT calculations

As mentioned earlier, As and Sb atoms tend to interact with vacancies in order to release the compressive strain and as such they form effective trapping centers for vacancies. To assess the possibility of trapping vacancies by dopant atoms, DFT calculations are used to calculate the binding energies of dopant-vacancy (DV) complexes. A similar method is hereby used as was used by Chronopoulos *et al.* to calculate carbon, dopant, and vacancy interactions in germanium and silicon.²³

Due to the presence of a relatively high concentration of O_i atoms in Cz silicon, the interaction between the dopant and O_i atoms leading to dopant- O_i (DO) complexes has to be considered as well as the further trapping of O_i atoms by DV pairs thus forming dopant-vacancy- O_i (DVO) complexes.

For simplicity, only the most energetically favorable configurations of DV, DO, and DVO complexes are shown in Fig. 4, as obtained by the DFT calculations in the present study and also reported by others.²⁴ In the case that a dopant atom binds with a vacancy, the vacancy locates at the first nearest lattice site of the dopant atom to form the most stable DV complex. When an interstitial oxygen atom binds with a dopant atom, it tends to be in the bond interstitial site of two

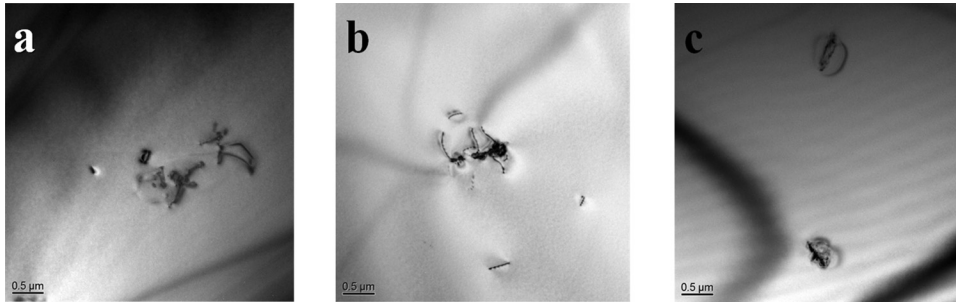


FIG. 1. TEM images illustrating typical BMDs in (a) As-doped Cz silicon and (b) Sb-doped Cz silicon specimens, after a thermal treatment at 800 °C for 32 h + 1000 °C for 32 h, (c) Sb-doped Cz silicon specimens annealed at 900 °C for 32 h. All specimens received a prior RTP at 1250 °C for 60 s.

neighboring silicon atoms which are the second and third next nearest neighbors of the dopant atom, respectively. To form a DVO complex, an O_i atom is added to an existing DV pair by compensating the two dangling bonds caused by the vacancy.

1. Binding energies of DV, DO, and DVO

The calculated binding energies of the three complexes as mentioned above are listed in Table I resulting from

calculation with constant volume and with constant zero pressure. The binding energy (E_b) of a dopant-incorporating complex is hereby calculated according to

$$E_b = E[\text{complex}] - \Sigma E[\text{isolated defect}] + nE[\text{perfect}] (n = 1 \text{ or } 2), \quad (1)$$

where $E[\text{complex}]$, $E[\text{isolated defect}]$, and $E[\text{perfect}]$ represent the total energies of a supercell containing a complex, one containing an isolated dopant atom or vacancy, and a

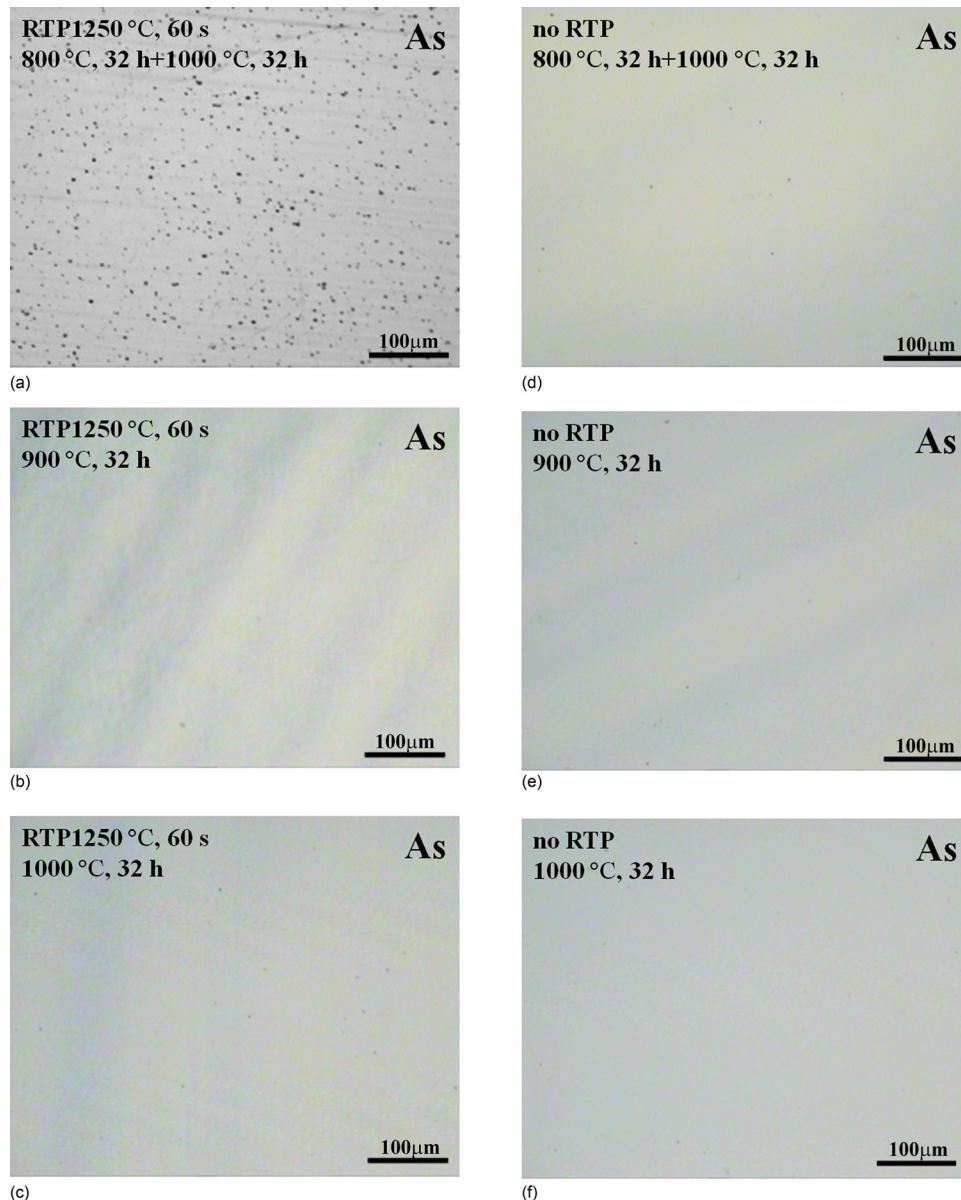


FIG. 2. Typical OM images of BMDs observed after preferential etching of As-doped specimens subjected to anneals at 800 °C for 32 h + 1000 °C for 32 h, at 900 °C for 32 h, and at 1000 °C for 32 h, with (right column) and without (left column) a prior RTP at 1250 °C for 60 s, respectively.

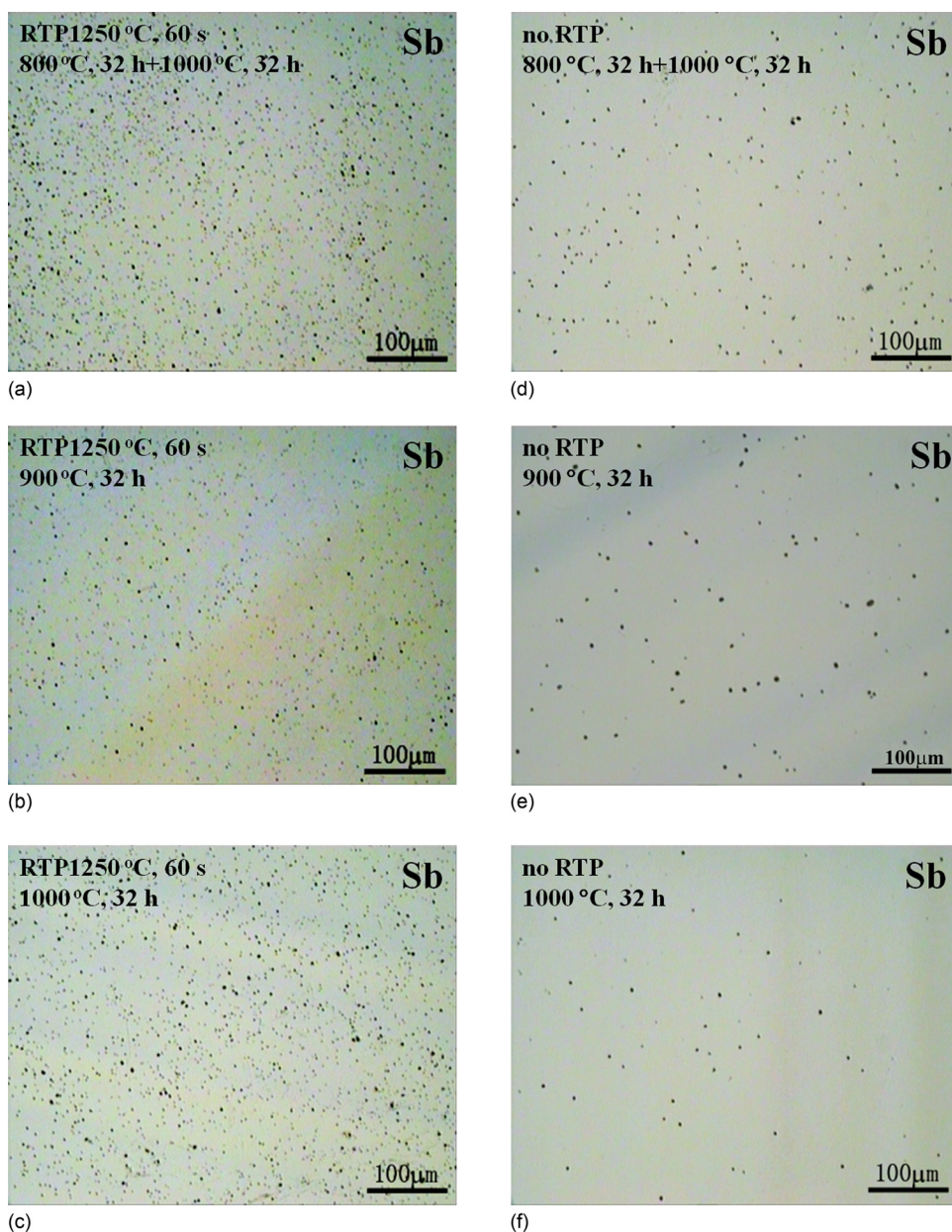


FIG. 3. Typical OM images of BMDs observed after preferential etching of Sb-doped Cz silicon specimens subjected to anneals at 800 °C for 32 h + 1000 °C for 32 h, at 900 °C for 32 h, and at 1000 °C for 32 h, with (right column) and without (left column) a prior RTP at 1250 °C for 60 s, respectively.

perfect supercell without any defects, respectively. When E_b is negative, it means that the complex is more stable than the isolated defects that are forming the complex.

According to the calculated binding energies, As and Sb atoms will indeed tend to combine with the vacancy to form the DV pair, confirming that substitutional dopant atoms with larger size than silicon atoms will act as vacancy traps. Moreover, the binding energy of a SbV pair is larger than that of an AsV pair showing that, as expected, a dopant atom with a larger size is a more effective trap for a vacancy.

In comparison with DV pairs, the DO pairs have remarkably smaller binding energies. As listed in Table I, the AsO pair has a binding energy of only -0.17 eV, while the SbO pair even has a slightly positive binding energy and should therefore be unstable. It can be concluded that the formation of AsO and SbO pairs is energetically less favorable than the formation of AsV and SbV pairs. However, if an O_i atom attaches to the vacancy side of a DV pair, the new DVO complex has a considerably larger binding energy, reaching

-2.86 and -3.08 eV for the AsVO and SbVO complexes, respectively. Similar to the case of the DV pair, the binding energy of the DVO complex increases with the dopant atom size. The large binding energies as mentioned above imply that once the AsVO and SbVO complexes form in As- or Sb-doped Cz silicon, they will be relatively stable even at more elevated temperatures.

In Cz silicon, O_i atoms themselves can also act as vacancy traps. In lightly doped Cz silicon, the more mobile vacancies are captured by O_i atoms, forming relatively stable VO pairs that further trap O_i atoms and evolve into VO_2 complexes. Such VO_2 complexes are considered to be the precursors of heterogeneous nucleation of oxide precipitates.^{2,9,10} For As or Sb-doped Cz silicon, as mentioned above, As and Sb atoms can trap vacancies to form AsV and SbV complexes and, furthermore, these DV pairs can also capture O_i atoms to evolve into AsVO and SbVO complexes. Due to the competition with the dopant atoms acting as traps for vacancies especially in the case of heavily doped material

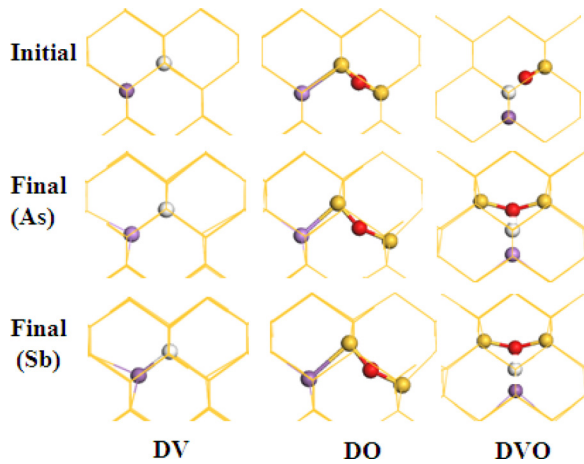


FIG. 4. Configurations of DV, DO, and DVO complexes before and after structure relaxation in As or Sb doped silicon. The yellow, blue, white, and red balls represent a silicon atom, a dopant (As or Sb) atom, a vacancy and an oxygen atom, respectively.

with dopant concentrations exceeding that of O_i , the formation of VO and VO_2 complexes will inevitably be influenced by the doping.

2. Estimating the vacancy capturing strength of D and O_i

To obtain a better understanding of the effect of As- or Sb-doping on the formation of VO complexes in Cz silicon, the vacancy-capture capabilities of As, Sb, and O_i are compared. A simple model in which an As or Sb atom and an O_i atom coexist in a 128-atom supercell is built. For convenience, the vacancy is initially introduced at the midpoint between the As or Sb atom and O_i as shown schematically in Fig. 5. The reference state is defined when the vacancy is located at infinity. The energy difference between the final state (with the vacancy at the different NN sites) and the reference state (where dopant atom and O_i already coexist with the vacancy at infinity) is calculated as was also done in a study of the effect of Sn on point defects and oxygen precipitation in Cz silicon.²⁵

The results of this calculation are summarized in Table II. When the vacancy is progressively closer to the As or Sb atom, the absolute value of the energy difference increases. This results from the partial release of the As- or Sb-atom induced compressive strain by the vacancy. This scenario is

TABLE I. Binding energies in eV of DV, DO, and DVO complexes calculated under constant lattice parameter (0.543 nm) (top) and under constant zero pressure conditions (bottom).

Constant volume			
D	DV	DO	DVO
As	-1.30	-0.17	-2.86
Sb	-1.57	0.01	-3.08
Constant pressure			
D	DV	DO	DVO
As	-1.32	-0.12	-2.34
Sb	-1.50	0.01	-2.29

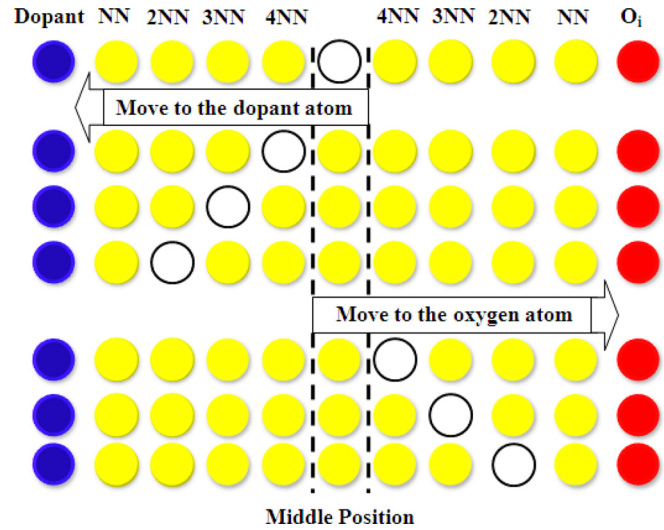


FIG. 5. Schematic representation of the movement of a vacancy towards a substitutional dopant atom or an interstitial oxygen atom. Initially, the vacancy is in the middle between the dopant and the oxygen atom. The total energy and the binding energy are calculated in each nearest neighbor position.

repeated for the movement of the vacancy towards O_i showing that the absolute value of the energy difference when forming the VO pair is somewhat higher than when forming the AsV or SbV pair.

At first sight, it seems contradictory that the VO binding energy is larger than the VD binding energy and still the VD pairs are more easily formed than the VO pairs. The reason for this is the energy difference listed in Table II which is larger for the VD pairs than for the VO pair. The larger binding energy of the VO pair is mainly due to dangling bond compensation which does not occur when forming a VD pair. Before this dangling bond compensation, the energy difference is only due to stress differences and the data in Table II reflect the capture efficiency between O_i and D.

Therefore, according to the aforementioned theoretical calculations, it can be assumed that the As and Sb atoms have a vacancy-capture capability that is comparable to that of the O_i atom.

3. Comparing the As- and the Sb-doped material of the present study

The concentration of As atoms is more than one order of magnitude higher than that of O_i . As a consequence, the

TABLE II. Energy difference in eV due to introduction of a vacancy calculated for constant zero pressure as function of the position of the vacancy with respect to the dopant (As or Sb) or the O_i atom as schematically shown in Fig. 5.

	Middle	4NN	3NN	2NN
O_i	-0.32	-0.26	-0.27	-1.33
As	-0.32	-0.26	-0.39	-1.39
	Middle	4NN	3NN	2NN
O_i	-0.26	-0.23	-0.29	-1.32
Sb	-0.26	-0.33	-0.42	-1.43

diffusing vacancies encounter the As atoms more frequently than the O_i atoms, resulting in a higher probability of forming the AsV pairs and subsequently also the AsVO complexes. Furthermore, the O_i atoms diffuse a great deal faster than the substitutional As or Sb atoms that can be considered as being immobile in comparison. Therefore, unlike the AsV and SbV complexes, the VO complexes are remarkably mobile even at relatively low temperatures as is known from irradiation experiments followed by low temperature thermal anneals.

Besides the divacancy and the E-center (or DV-center) in n-type Si, the VO-center (or A-center), is one of the main defects introduced in oxygen-rich Cz Si by irradiation. As the VO-center already becomes unstable at 300 °C, it can also be expected that it is already mobile at these temperatures, whereby the dopant and even the interstitial oxygen atoms can be considered as being immobile.^{26,27} In fact, a whole family of V_xO_y -centers develops during rapid cooling and subsequent thermal anneals with a continuously changing distribution of the different vacancy-oxygen complexes.²⁸

It has been reported that As can also diffuse via an interstitial mechanism in case a large supersaturation of interstitials exists which is the case after ion implantation^{29–31} but as the vacancy is the dominant intrinsic point defect in RTP treated as-grown wafers, this possibility is not considered further. A part of the VO complexes will therefore be inevitably captured by the As or Sb atoms, resulting in the formation of AsVO or SbVO complexes. Depending on the As or Sb concentration, it can even be expected that the formation of AsVO or SbVO complexes prevails over that of VO_2 complexes.

C. A tentative model for the OP behavior in low resistivity As- and Sb-doped silicon

According to the DFT calculations discussed above, the AsV and SbV pairs are quite stable due to their large binding energies. During the RTP at high temperatures, vacancies tend to form at the first nearest neighbors of Sb or As atoms in order to partially release the compressive strain in the silicon lattice.³² These vacancies are trapped by the dopant atom leading to the formation of DV pairs. As the As concentration is approximately 20 times higher than the Sb concentration, it can be expected that the concentration of AsV pairs is proportionally higher than that of SbV pairs as can be estimated based on a simple continuum model and is also confirmed by measuring the resistivity change after RTP.^{33,34} Due to the capturing of vacancies generated during the RTP treatment by dopant atoms, the resistivity of the samples indeed increases by deactivation of dopant atoms. Assuming that the free carrier decrease is due to the formation of dopant-vacancy pairs, the total vacancy concentration in the As and in the Sb doped samples can be estimated to be about $3\text{--}5 \times 10^{17} \text{ cm}^{-3}$ and $4 \times 10^{16} \text{ cm}^{-3}$, respectively.³⁵ These concentrations of dopant-vacancy pairs are 4 and 3 orders of magnitude higher than the thermal equilibrium concentration of neutral vacancies at 1250 °C which is about $3.7 \times 10^{13} \text{ cm}^{-3}$ at 1250 °C.³⁴ A more extended report on

this change of resistivity and its recovery during low temperature anneals will be published elsewhere.

Similar trapping effects due to dopant-vacancy pair formation have been reported for Si doped with high concentrations of isovalent impurities Ge³⁶ and Sn.^{25,37} Heavy doping with Ge also leads to an apparent decrease of the formation energy of the vacancy which was shown to be due to the total vacancy increase during a high temperature anneal by the trapping effect.³⁵

An important difference is however that in heavily As and Sb doped Si, also the formation energy of the double negatively charged vacancy is considerably lowered and is much lower than that of the neutral vacancy.³⁴ Due to this lower formation energy, the free and trapped vacancy concentration is significantly higher than in Si doped with isovalent impurities, and therefore, also the effects on BMD nucleation are larger.

Although the trapping has a negligible effect on the thermal equilibrium concentration of vacancies, the total number of vacancies can thus increase orders of magnitude and the formed DV pairs form a huge reservoir of vacancies that can be released during subsequent thermal treatments when the DV pairs become unstable. During the cooling down part of the RTP and especially at the initial stage of the subsequent annealing at 800–1000 °C, O_i atoms diffuse toward the AsV or SbV pairs to form AsVO or SbVO complexes, respectively, which are quite stable at the annealing temperature due to their considerably larger binding energy as listed in Table I. With the incorporation of more O_i atoms, the AsVO or SbVO complexes are assumed to evolve into oxide precipitate nuclei. If these nuclei are larger than the critical size corresponding to the specific annealing temperature, they are stable and can grow further into oxide precipitates observed as BMDs. It is well known that the critical size beyond which the above-mentioned nuclei can grow into oxide precipitates increases with annealing temperature and compressive stress and decreases with increasing oxygen content and vacancy supersaturation.³⁸ As the difference in oxygen content between the wafers used in the present study is rather small, the change of the vacancy supersaturation after RTP will dominate the critical precipitate size. The comparison between the As- and Sb-doped Cz silicon crystals of the present study suggests that, on the average, more O_i atoms are aggregating into SbVO complexes than in AsVO complexes. Oxide precipitate nucleation and growth can occur during the annealing at 900 or 1000 °C in the Sb-doped Cz silicon as less RTP generated vacancies are trapped by the Sb atoms and more vacancies thus remain available to reduce the critical size of the oxide precipitates.

This is in contrast to the case of the As-doped samples, as shown in Figs. 2 and 3. Nevertheless, as shown in Fig. 2, OP during the two-step anneal at 800 °C for 32 h + 1000 °C for 32 h in the As-doped Cz silicon is also enhanced by the prior RTP at 1250 °C. For the same oxygen content and vacancy concentration, the critical size for homogeneous oxide precipitate nucleation is smaller at 800 °C than at 900 or 1000 °C. Therefore, more of the AsVO-complexes can evolve into oxide precipitate nuclei during the 800 °C anneal and then further grow during the subsequent 1000 °C anneal.

V. CONCLUSIONS

The OP behavior is experimentally investigated in heavily As- or Sb-doped Cz silicon crystals subjected to two-step anneals at 800 °C for 32 h + 1000 °C for 32 h, or single-step anneals for 32 h at 900 or 1000 °C with and without a prior RTP at 1250 °C. It is found that the prior RTP enhances OP in all cases for the Sb-doped Cz silicon but only for the two-step anneal in case of the As-doped silicon.

DFT calculations indicate that it is energetically favorable to form AsVO and SbVO complexes, whereby the SbVO complex has a larger binding energy. As the concentration of As and Sb is larger than that of O_i, and as also the binding energy of the dopants with vacancies is much larger than that with oxygen, the formation of AsV or SbV pairs is favored over that of VO and VO₂ complexes. Such AsVO and SbVO complexes are assumed to be precursors for the formation of oxide precipitate nuclei during subsequent anneals. Due to the extensive vacancy trapping in the As doped samples, at the same time the oxide precipitate critical size is considerably larger than in the Sb doped samples despite the somewhat higher O_i content in the As doped material.

The present results show that RTP can be used to enhance OP and therefore the IG capability of epitaxial silicon wafers using heavily As- or Sb-doped substrates. At the same time, one should be aware of the vacancy trapping effect that increases strongly with dopant concentration and thus reduces the beneficial effect of the RTP step.

ACKNOWLEDGMENTS

The authors acknowledge the financial support from Natural Science Foundation of China (No. 50832006), National Science and Technology Major Project (No. 2010ZX02301-003), Zhejiang provincial Natural Science Fund (No. R4090055), Innovation Team Project of Zhejiang Province (No. 2009R50005), and FWO (project VS.040.11 N). Shanghai Super Computer Center is acknowledged for providing computation resources for the DFT calculations. Maosen Fu acknowledges the financial support from the State Key Laboratory of Silicon Materials, Zhejiang University.

¹A. Borghesi, B. Pivac, A. Sassella, and A. Stella, *J. Appl. Phys.* **77**, 4169 (1995).

²R. Falster, V. V. Voronkov, and F. Quast, *Phys. Status Solidi B* **222**, 219 (2000).

³X. Ma, L. Lin, D. Tian, L. Fu, and D. Yang, *J. Phys.: Condens. Matter* **16**, 3563 (2004).

⁴R. Falster and V. V. Voronkov, *Mater. Sci. Eng., B* **73**, 87 (2000).

⁵V. V. Voronkov and R. Falster, *Mater. Sci. Semicond. Process.* **5**, 387 (2002).

⁶R. Falster, M. Pagani, D. Gambaro, M. Cornara, M. Olmo, G. Ferrero, P. Pichler, and M. Jacob, *Solid State Phenom.* **57–58**, 129 (1997).

⁷R. Falster, M. Cornara, D. Gambaro, M. Olmo, and M. Pagani, *Solid State Phenom.* **57–58**, 123 (1997).

⁸M. Pagani, R. Falster, G. R. Fisher, G. C. Ferrero, and M. Olmo, *Appl. Phys. Lett.* **70**, 1572 (1997).

⁹G. Kissinger, J. Dabrowski, A. Sattler, C. Seuring, T. Müller, H. Richter, and W. von Ammon, *J. Electrochem. Soc.* **154**, H454 (2007).

¹⁰V. V. Voronkov and R. Falster, *J. Electrochem. Soc.* **149**, G167 (2002).

¹¹F. S. d'Aragona and P. L. Fejes, *Appl. Phys. Lett.* **48**, 665 (1986).

¹²T. Nozaki, Y. Itoh, T. Masui, and T. Abe, *J. Appl. Phys.* **59**, 2562 (1986).

¹³S. K. Bains, D. P. Griffiths, J. G. Wilkes, R. W. Series, and K. G. Barraclough, *J. Electrochem. Soc.* **137**, 647 (1990).

¹⁴B. Wang, X. Zhang, X. Ma, and D. Yang, *J. Cryst. Growth* **318**, 183 (2011).

¹⁵Y. Zhao, D. Li, X. Ma, and D. Yang, *J. Phys.: Condens. Matter* **16**, 1539 (2004).

¹⁶M. D. Segall, P. J. D. Lindan, M. J. Probert, C. J. Pickard, P. J. Hasnip, S. J. Clark, and M. C. Payne, *J. Phys.: Condens. Matter* **14**, 2717 (2002).

¹⁷P. E. Blöchl, *Phys. Rev. B* **50**, 17953 (1994).

¹⁸D. Vanderbilt, *Phys. Rev. B* **41**, 7892 (1990).

¹⁹J. Perdew, K. Burke, and M. Ernzerhof, *Phys. Rev. Lett.* **77**, 3865 (1996).

²⁰H. J. Monkhorst and J. D. Pack, *Phys. Rev. B* **13**, 5188 (1976).

²¹J. Vanhellemont, O. De Gryse, and P. Clauws, *Phys. Status Solidi A* **203**, 2341 (2006).

²²J. Vanhellemont, O. De Gryse, and P. Clauws, *Appl. Phys. Lett.* **86**, 221903 (2005).

²³A. Chronos, B. P. Uberuaga, and R. W. Grimes, *J. Appl. Phys.* **102**, 083707 (2007).

²⁴A. Chronos, E. N. Sgourou, and C. A. Londos, *J. Appl. Phys.* **112**, 073706 (2012).

²⁵C. Gao, X. Ma, J. Zhao, and D. Yang, *J. Appl. Phys.* **113**, 093511 (2013).

²⁶M.-A. Trauwaert, J. Vanhellemont, H. E. Maes, A.-M. Van Bavel, G. Langouche, and P. Clauws, *Appl. Phys. Lett.* **66**, 3056 (1995).

²⁷G. D. Watkins, *Mater. Sci. Semicond. Process.* **3**, 227 (2000).

²⁸G. Kissinger, J. Dabrowski, D. Kot, V. Akhmetov, A. Sattler, and W. von Ammon, *J. Electrochem. Soc.* **158**, H343 (2011).

²⁹S. Solmi, M. Ferri, M. Bersani, D. Giubertoni, and V. Soncini, *J. Appl. Phys.* **94**, 4950 (2003).

³⁰S. A. Harrison, T. F. Edgar, and G. S. Hwang, *Appl. Phys. Lett.* **87**, 231905 (2005).

³¹S. A. Harrison, T. F. Edgar, and G. S. Hwang, *Phys. Rev. B* **74**, 195202 (2006).

³²J. Xie and S. P. Chen, *J. Appl. Phys.* **87**, 4160 (2000).

³³X. Zhang, X. Ma, C. Gao, T. Xu, J. Zhao, P. Dong, D. Yang, and J. Vanhellemont, *ECS Trans.* **52**(1), 683 (2013).

³⁴J. Vanhellemont, E. Kamiyama and K. Sueoka, *ECS J. Solid State Sci. Technol.* **2**, P166 (2013).

³⁵J. Vanhellemont, M. Suezawa, and I. Yonenaga, *J. Appl. Phys.* **108**, 016105 (2010).

³⁶C. A. Londos, A. Andrianakis, V. V. Emtsev, and H. Ohyama, *Semicond. Sci. Technol.* **24**, 075002 (2009).

³⁷C. Claeys, E. Simoen, V. B. Neimash, A. Kraitichinskii, M. Kras'ko, O. Puzenko, A. Blondeel, and P. Clauws, *J. Electrochem. Soc.* **148**, G738 (2001).

³⁸J. Vanhellemont and C. Claeys, *J. Appl. Phys.* **62**, 3960 (1987); J. Vanhellemont and C. Claeys, *ibid.* **71**, 1073 (1992).